Highly selectivity and sensitivity Zn(II) coordination polymer luminescent sensor for Al^{3+} and NACs in aqueous phase

Xiao Zhang‡*[a], Xuan Luo‡[a], Nanxi Zhang[c], Jie Wu**[b], Yong-Qing Huang[d]

Supporting information

Figure cation:

Table cation:

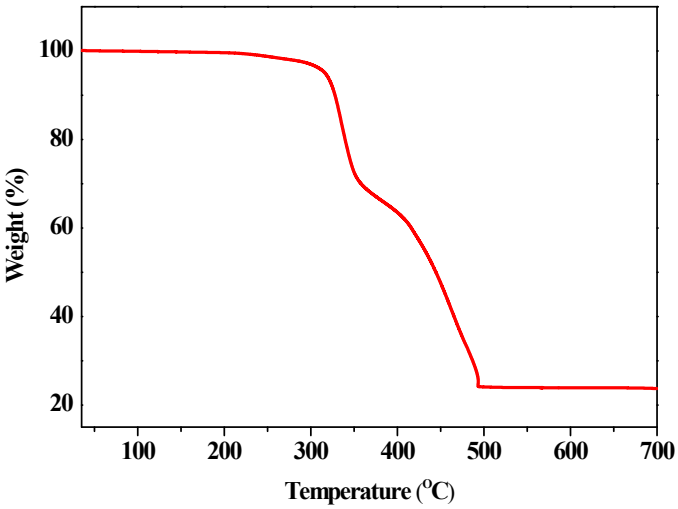

Fig.S1 The TGA plots of compound **1**

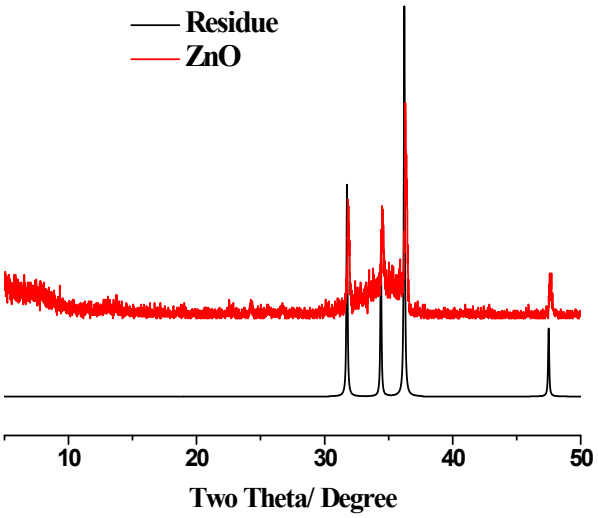

Fig.S2 Powder X-ray diffraction patterns for ZnO and residue of compound **1** after thermogravimetric analysis.

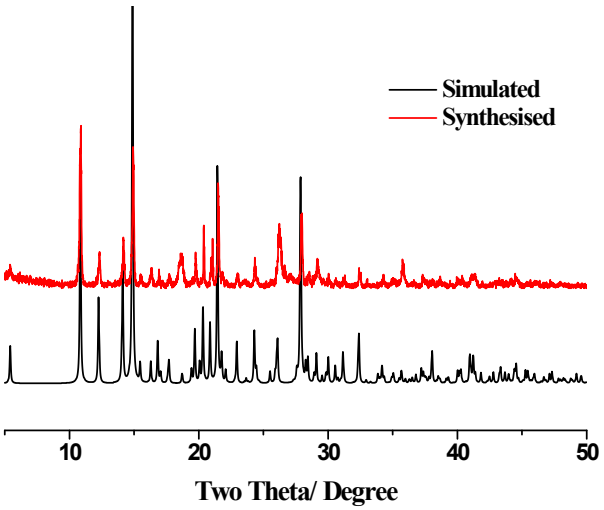

Fig. S3 Experimental and simulated Powder X-ray diffraction patterns for compound **1.**

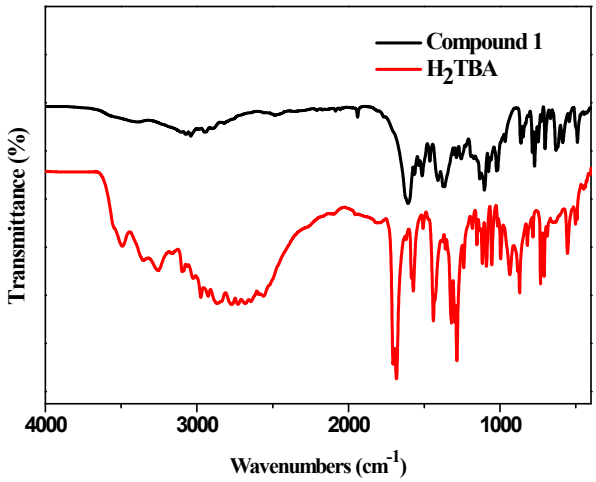

Fig. S4 IR spectra of compound **1** and H_2TBA ligand

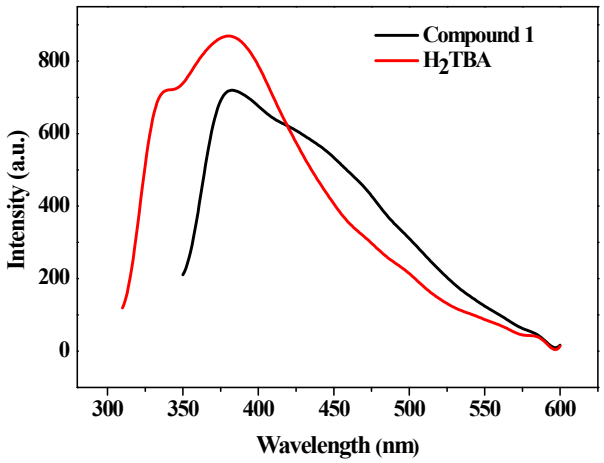

Fig. S5 Solid state emission spectra of compound **1** and free H_2TBA ligand upon excitation at 303 nm and 276 nm, respectively.

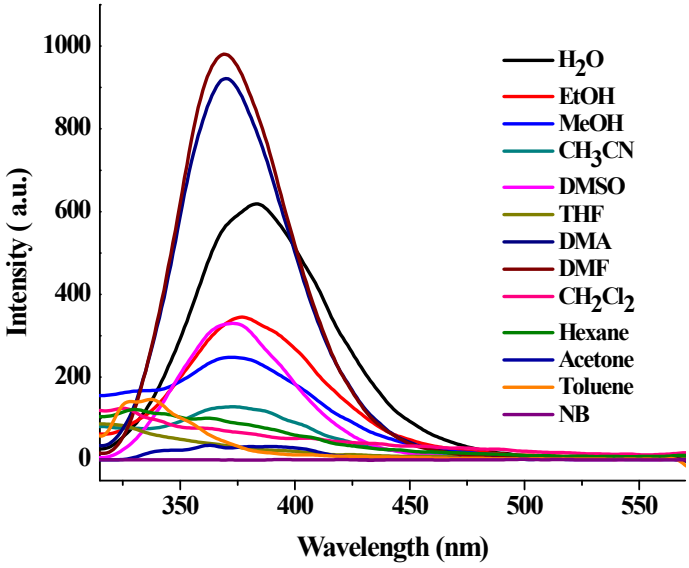

Fig S6 Emission spectra of **1** dispersed in different solvents when excited at 295 nm.

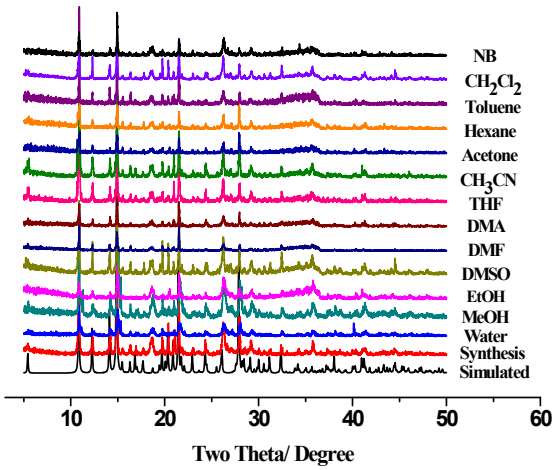

Fig. S7 Powder XRD patterns of **1** immersed in different solvents at room temperature.

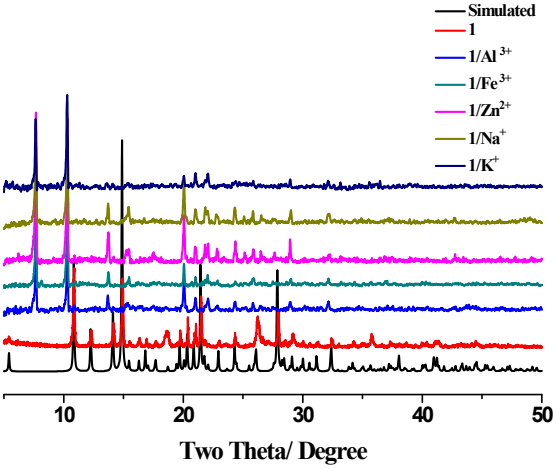

Fig. S8 Powder XRD patterns of simulated from the single-crystal data of **1** and synthesized compound and **1**/M^{n+}

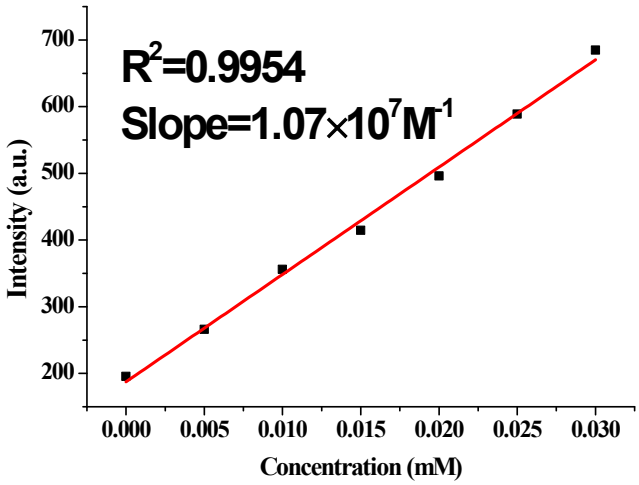

Linear Equation: Y = -10695X + 187.40 R = 0.9954

Slope = 1.070 × 10^7 M^{-1}

δ=4.21 (N=10)

Limit detection =3δ/Slope=7.18×10^{-6} M

Fig. S9 The fitting curve of the luminescence intensity of **1** at different Al^{3+} concentration

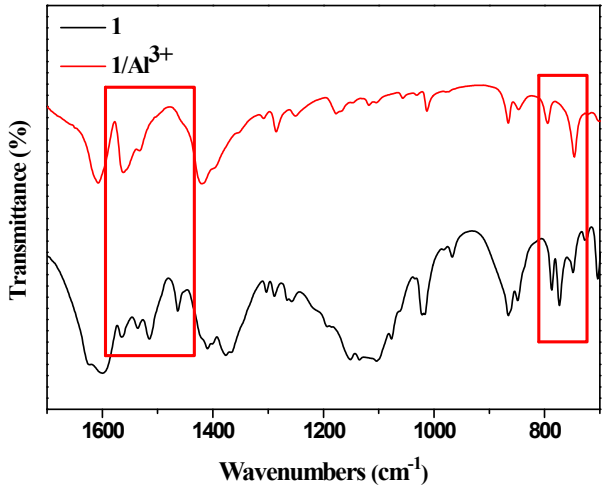

Fig. S10 IR spectra of compound **1** and **1/Al^{3+}**

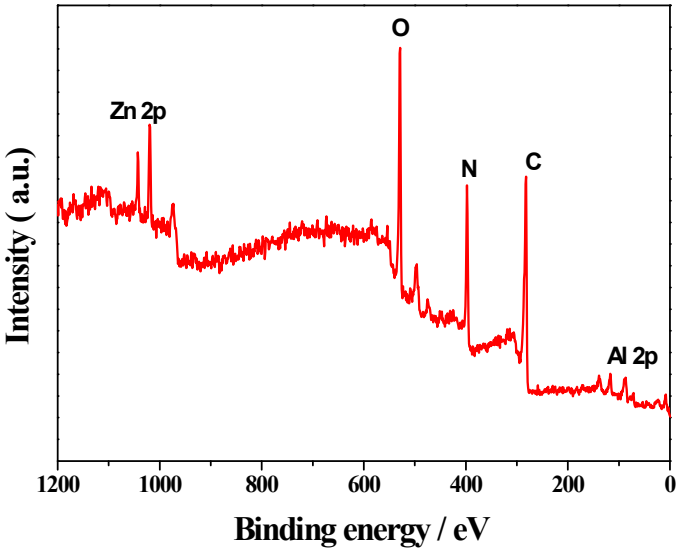

Fig. S11 The XPS of **1**/Al^{3+} shows the typical peak of Al^{3+} at 74.8 ev

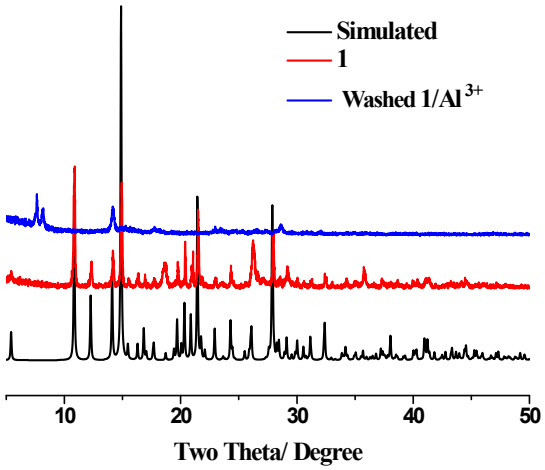

Fig. S12 Powder XRD patterns of simulated from the single-crystal data of **1** and synthesized compound and washed **1**/Al^{3+}.

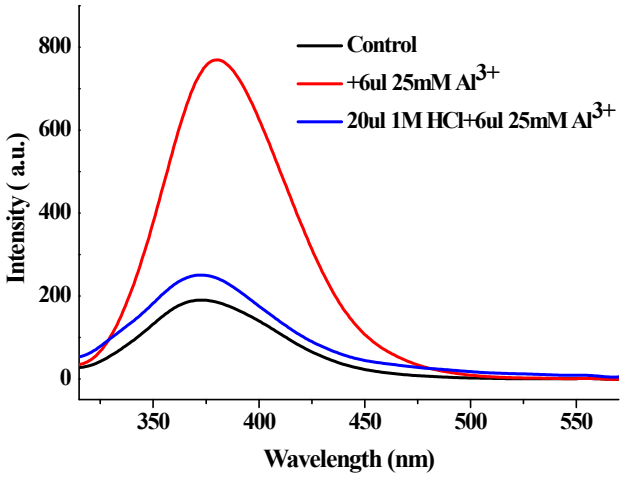

Fig. S13 The luminescence intensity of **1** upon incremental addition of Al^{3+} ions and addition of HCl and Al^{3+} ions, respectively.

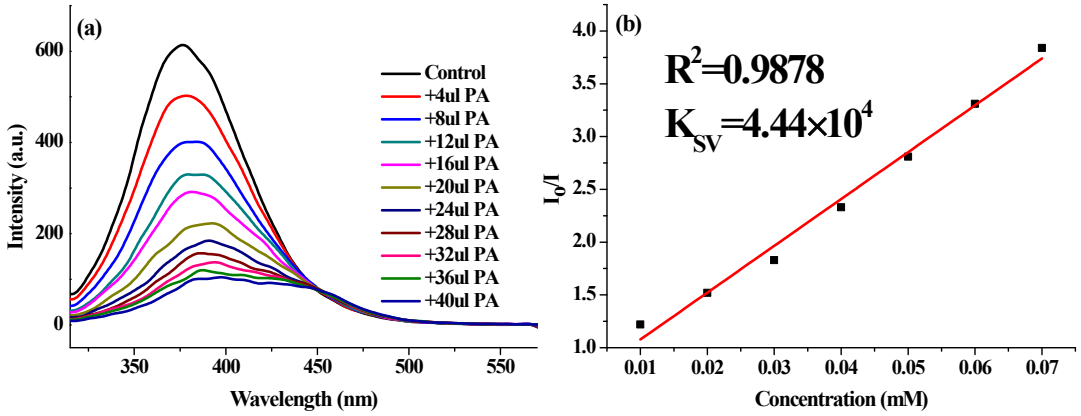

Fig.14 (a) The luminescence intensity of **1** upon incremental addition of PA solution (5 mM) in water. (b) Stern-Volmer plot for the luminescence intensity of **1** upon the addition of PA solution

(5 mM) in water.

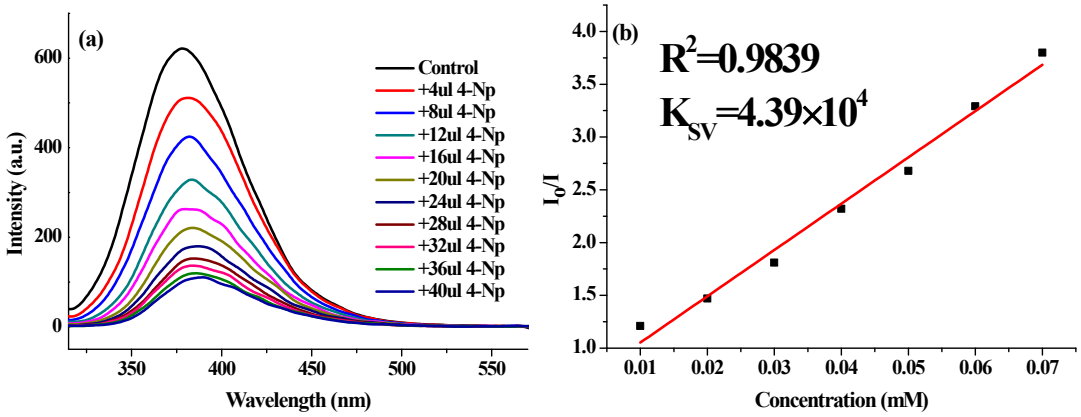

Fig.15 (a) The luminescence intensity of **1** upon incremental addition of 4-NP solution (5 mM) in water. (b) Stern-Volmer plot for the luminescence intensity of **1** upon the addition of 4-NP solution (5 mM) in water.

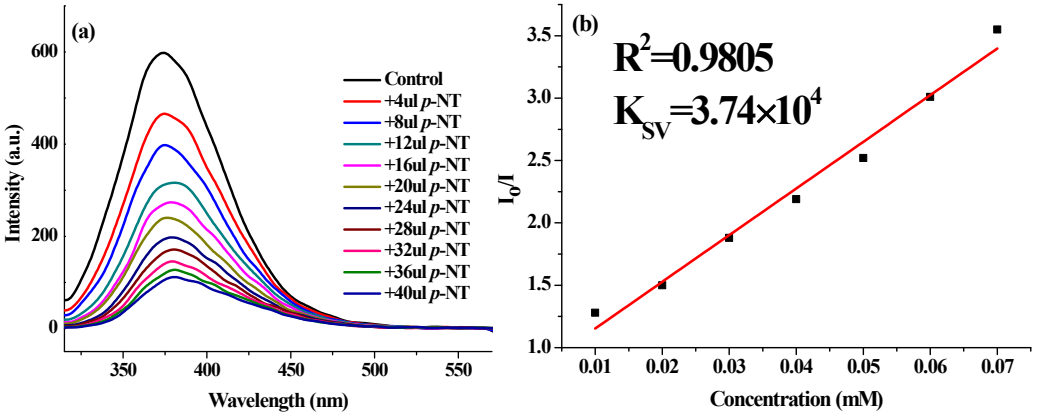

Fig.16 (a) The luminescence intensity of **1** upon incremental addition of *p*-NT solution (5 mM) in water. (b) Stern-Volmer plot for the luminescence intensity of **1** upon the addition of *p*-NT solution (5 mM) in water.

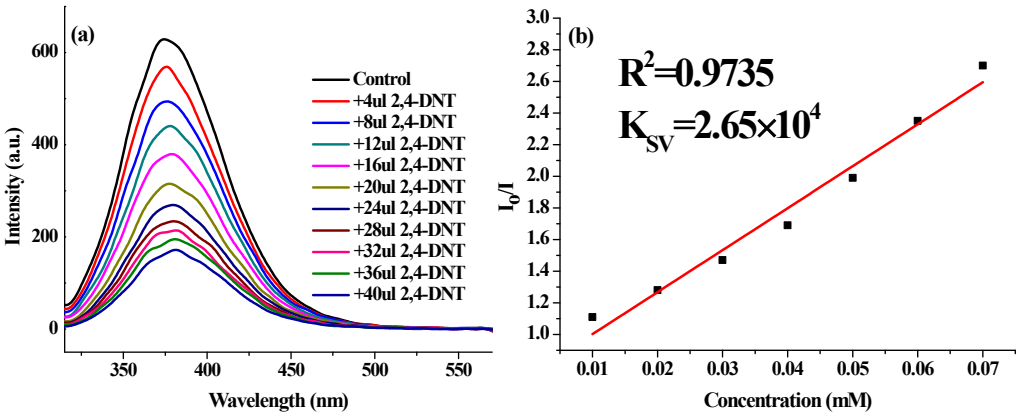

Fig.17 (a) The luminescence intensity of **1** upon incremental addition of 2,4-DNT solution (5 mM) in water. (b) Stern-Volmer plot for the luminescence intensity of **1** upon the addition of 2,4-DNT solution (5 mM) in water.

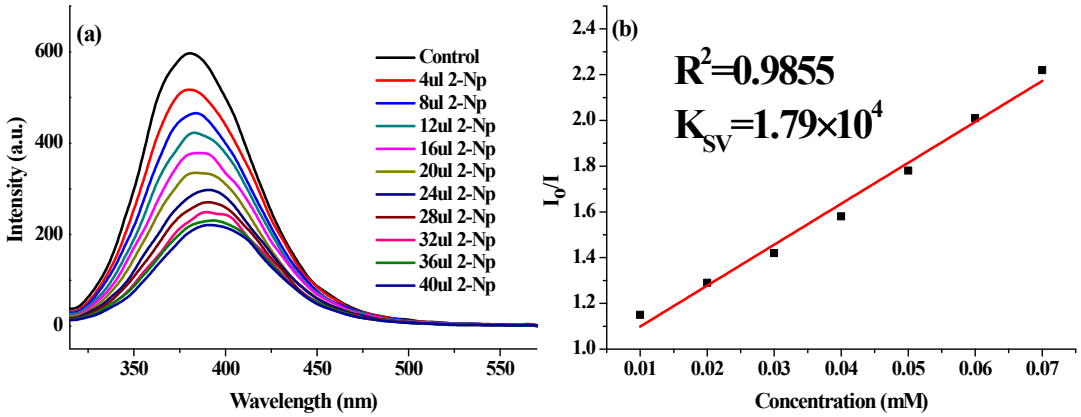

Fig.18 (a) The luminescence intensity of **1** upon incremental addition of 2-NP solution (5 mM) in water. (b) Stern-Volmer plot for the luminescence intensity of **1** upon the addition of 2 - NP solution (5 mM) in water.

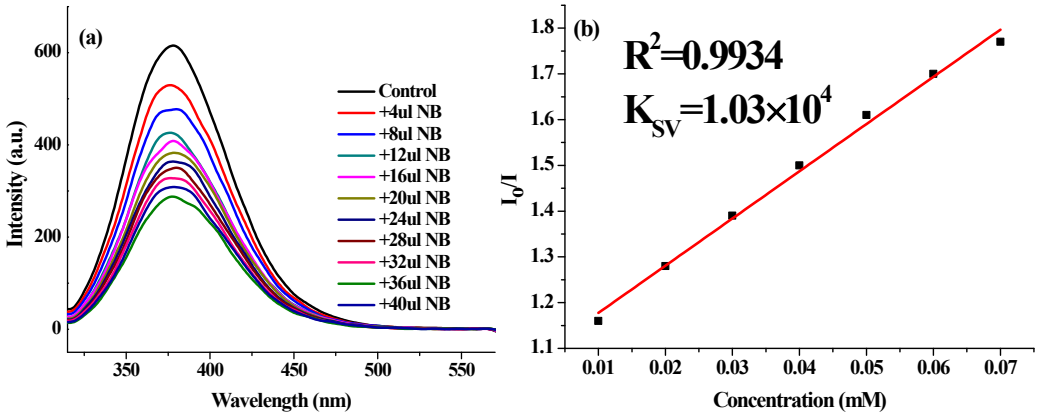

Fig.19 (a) The luminescence intensity of **1** upon incremental addition of NB solution (5 mM) in water. (b) Stern-Volmer plot for the luminescence intensity of **1** upon the addition of NB solution (5 mM) in water.

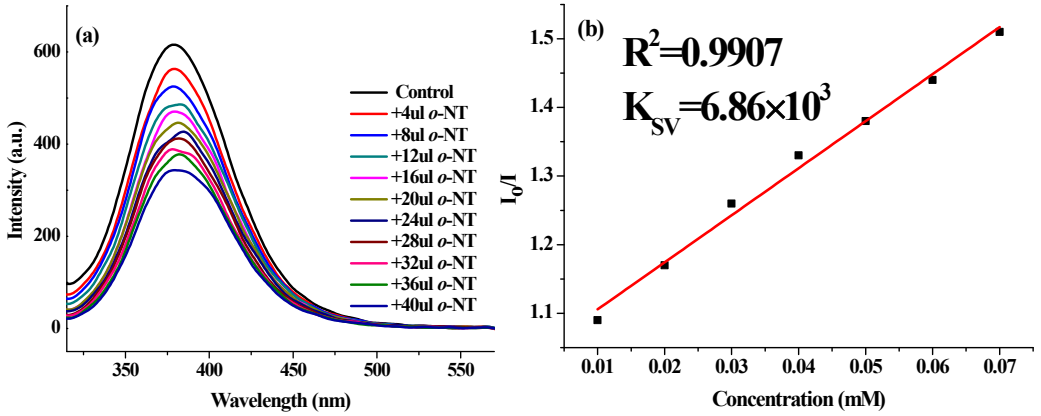

Fig. Fig.20 (a) The luminescence intensity of **1** upon incremental addition of *o*-NT solution (5 mM) in water. (b) Stern-Volmer plot for the luminescence intensity of **1** upon the addition of *o*-NT solution (5 mM) in water.

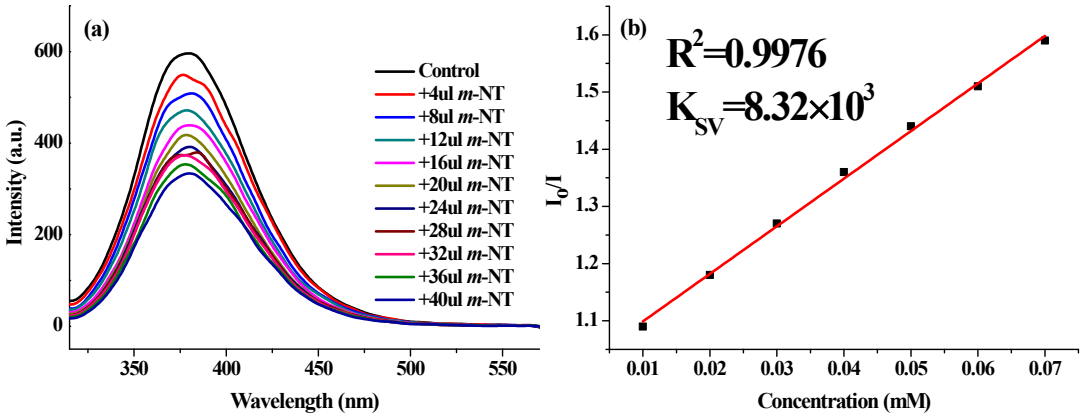

Fig.21 (a) The luminescence intensity of **1** upon incremental addition of *m*-NT solution (5 mM) in water. (b) Stern-Volmer plot for the luminescence intensity of **1** upon the addition of *m*-NT solution (5 mM) in water.

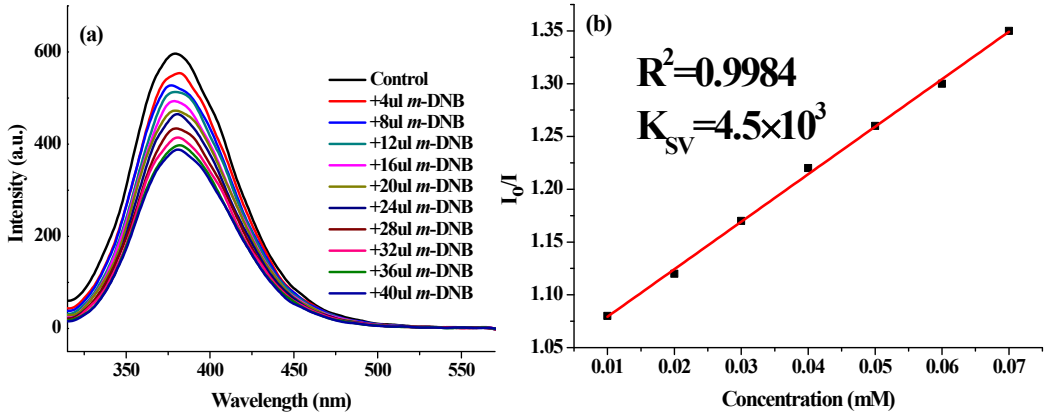

Fig.22 (a) The luminescence intensity of **1** upon incremental addition of *m*-DNB solution (5 mM) in water. (b) Stern-Volmer plot for the luminescence intensity of **1** upon the addition of *m*-DNB solution (5 mM) in water.

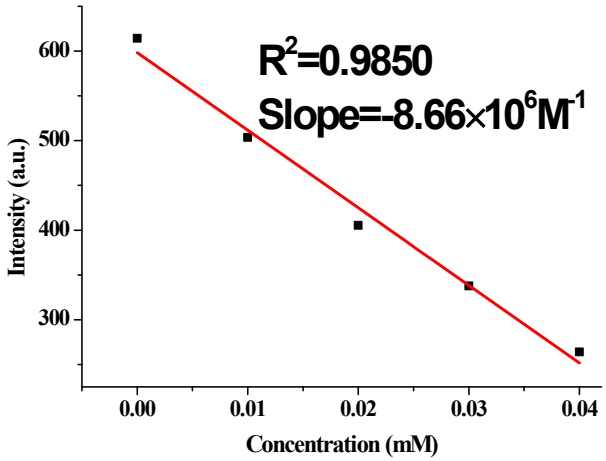

Linear Equation: Y = -8660X +598.22 R = 0.9850

Slope = 8.66× 10^6 M^{-1}

δ=4.21 (N=10)

Limit detection =3δ/Slope=1.46× 10^{-6} M

Fig. S23 The fitting curve of the luminescence intensity of **1** at different PA concentration (linear range 0-0.040 mM).

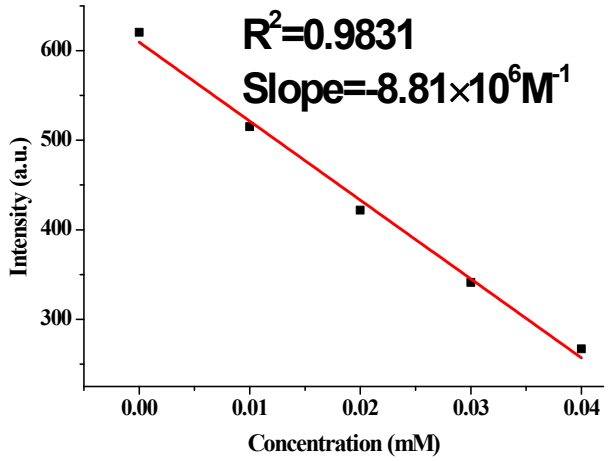

Slope = 8.81× 10^{6} M^{-1}

δ=4.21 (N=10)

Limit detection =3δ/Slope=1.43×10^{-6} M

Fig. S24 The fitting curve of the luminescence intensity of **1** at different 4-NP concentration (linear range 0-0.040 mM).

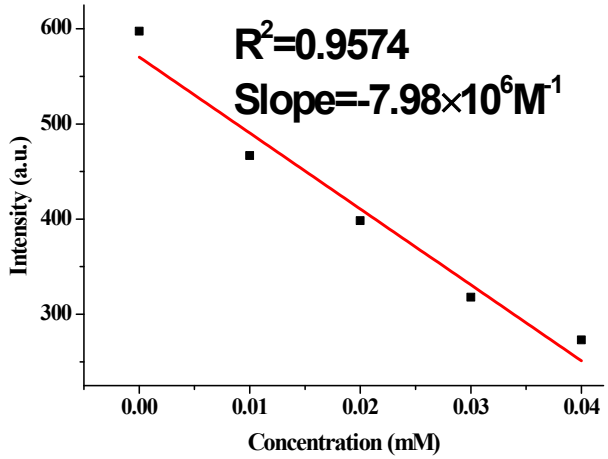

Slope = 7.98× 10^{6} M^{-1}

δ=4.21 (N=10)

Limit detection =3δ/Slope=1.58×10^{-6} M

Fig. S25 The fitting curve of the luminescence intensity of **1** at different *p*-NT concentration (linear range 0-0.040 mM).

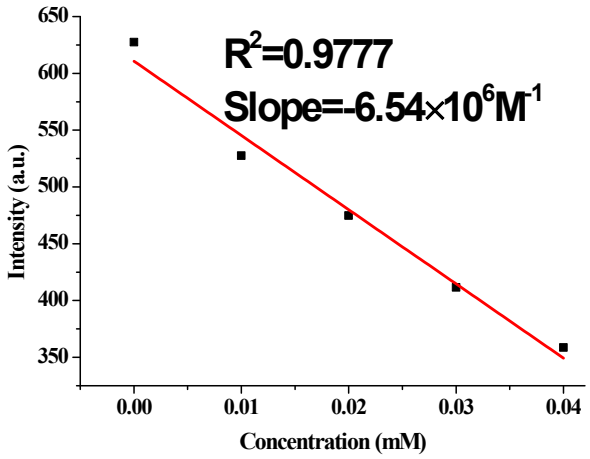

Slope = 6.54× 10^6 M^{-1}

δ=4.21 (N=10)

Limit detection =3δ/Slope=1.93×10^{-6} M

Fig. S26 The fitting curve of the luminescence intensity of **1** at different 2,4-DNT concentration (linear range 0-0.040 mM).

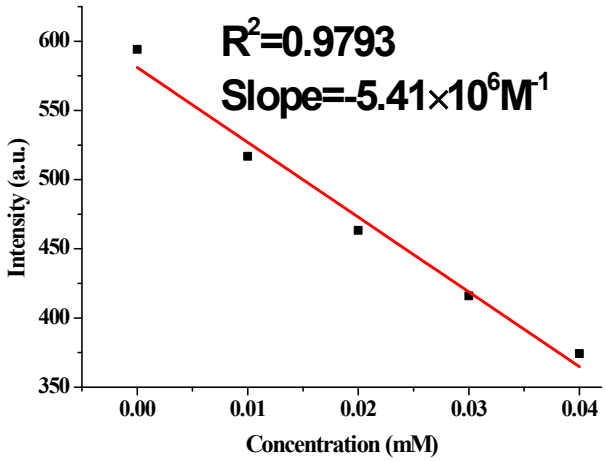

Slope = 5.41× 10^6 M^{-1}

δ=4.21 (N=10)

Limit detection =3δ/Slope=2.33×10^{-6} M

Fig. S27 The fitting curve of the luminescence intensity of **1** at different 2-Np concentration (linear range 0-0.040 mM).

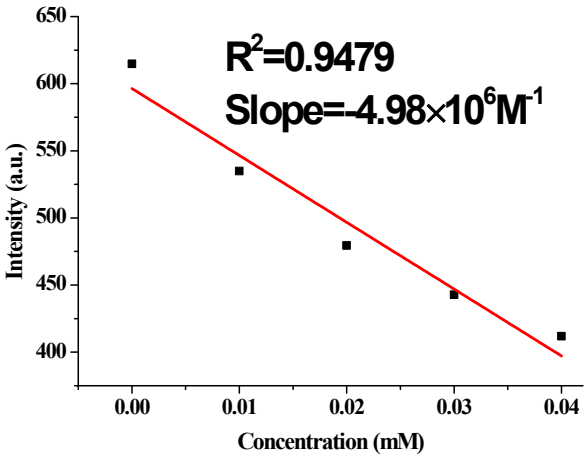

Slope = 4.98× 10^6 M^{-1}

δ=4.21 (N=10)

Limit detection =3δ/Slope=2.54×10^{-6} M

Fig. S28 The fitting curve of the luminescence intensity of **1** at different NB concentration (linear range 0-0.040 mM).

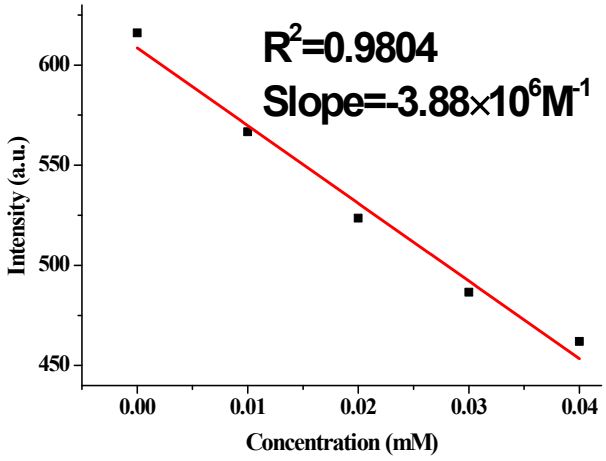

Slope = 3.88× 10^6 M^{-1}

δ=4.21 (N=10)

Limit detection =3δ/Slope=3.26×10^{-6} M

Fig. S29 The fitting curve of the luminescence intensity of **1** at different *o*-NT concentration (linear range 0-0.040 mM).

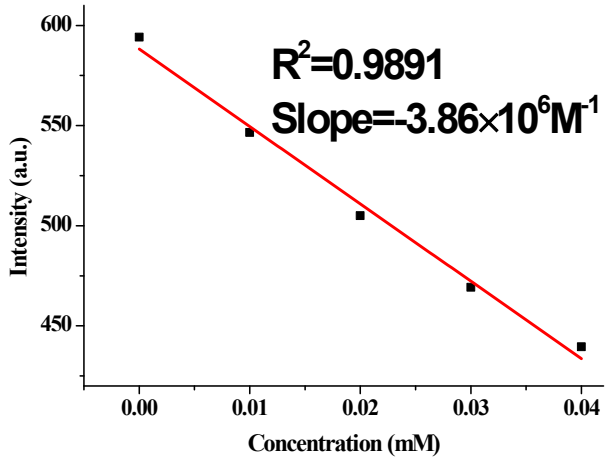

Slope = 3.86× 10^6 M^{-1}

δ=4.21 (N=10)

Limit detection =3δ/Slope=3.27×10^{-6} M

Fig. S30 The fitting curve of the luminescence intensity of **1** at different *m*-NT concentration (linear range 0-0.040 mM).

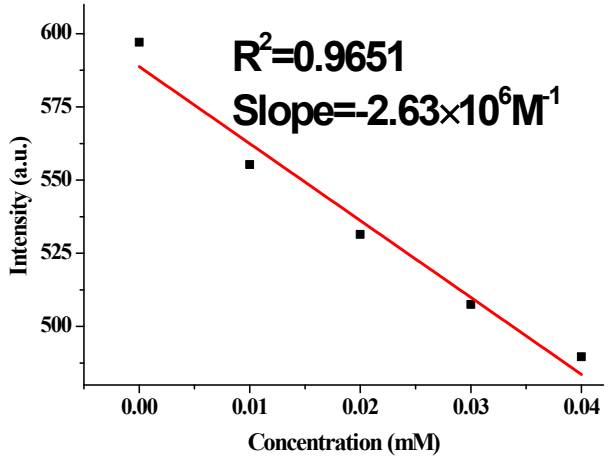

Slope = 2.63× 10^6 M^{-1}

δ=4.21 (N=10)

Limit detection =3δ/Slope=4.80×10^{-6} M

Fig. S31 The fitting curve of the luminescence intensity of **1** at different *m*-DNB concentration (linear range 0-0.040 mM).

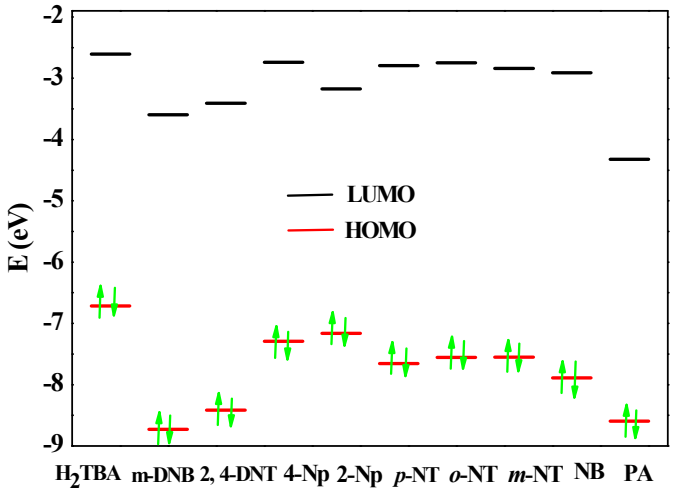

Fig. S32 HOMO and LUMO of H_2TBA ligand and NACs

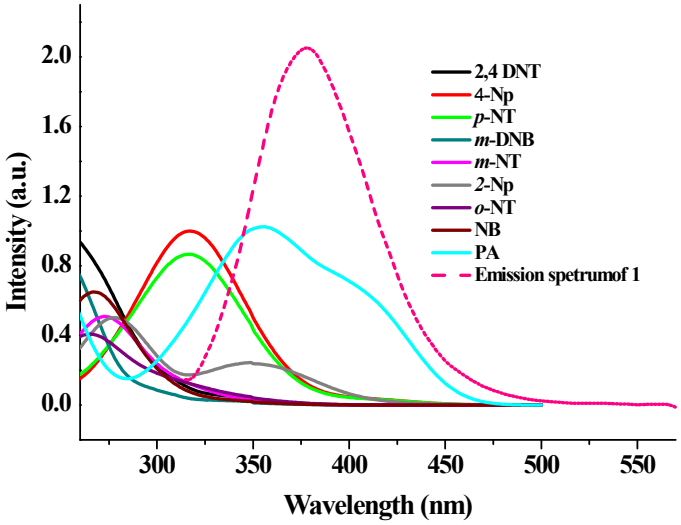

Fig. S33 Spectral overlaps between absorbance spectra of NACs and emission spectra of **1**.

Table S1**.** The Selected Bond Lengths (Å) and Angles (deg) of Compound **1**

Zn1-O1	1.920(2)	Zn1-O3	1.981(2)
Zn1-N1^{i}	2.033(3)	Zn1-N4^{ii}	2.015(3)
O1-Zn1-O3	124.76(11)	O1-Zn1-N1^{i}	104.44(12)
O1-Zn1-N4^{ii}	112.13(12)	O3-Zn1-N1^{i}	100.78(10)
O3-Zn1-N4^{ii}	103.05(11)	N4ii-Zn1-N1^{i}	110.92(11)

Symmetry codes: (i) 1/2+X,3/2-Y,1-Z; (ii) 1-X,1-Y,1-Z;

TableS2 HOMO and LUMO energies calculated for NACs and H_2TBA at B3LYP/6-31G* level of theory[1]

Analytes	Homo(ev)	LUmo(ev)	Bond gap

PA	-8.595166	-4.320934	4.274232
2,4-DNT	-8.41361	-3.409107	5.004502
p-NT	-7.655022	-2.792225	4.862798
NB	-7.887787	-2.912631	4.975156
m-DNB	-8.730522	-3.596104	5.134419
o-NT	-7.554773	-2.746777	4.807996
m-NT	-7.55031	-2.838932	4.711378
2-Np	-7.160373	-3.172671	3.987702
4-Np	-7.290064	-2.73967	4.550394
H_2TBA	-7.478068	-2.605952	5.034275

[1] M. J. Frisch, G. W. Trucks, H. B. Schlegel, G. E. Scuseria, M. A. Robb, J. R. Cheeseman, G. Scalmani, V. Barone, B. Mennucci, G. A. Petersson, H. Nakatsuji, M. Caricato, X. Li, H. P. Hratchian, A. F. Izmaylov, J. Bloino, G. Zheng, J. L. Sonnenberg, M. Hada, M. Ehara, K. Toyota, R. Fukuda, J. Hasegawa, M. Ishida, T. Nakajima, Y. Honda, O. Kitao, H. Nakai, T. Vreven, J. J. A. Montgomery, J. E. Peralta, F. Ogliaro, M. Bearpark, J. J. Heyd, E. Brothers, K. N. Kudin, V. N. Staroverov, T. Keith, R. Kobayashi, J. Normand, K. Raghavachari, A. Rendell, J. C. Burant, S. S. Iyengar, J. Tomasi, M. Cossi, N. Rega, J. M. Millam, M. Klene, J. E. Knox, J. B. Cross, V. Bakken, C. Adamo, J. Jaramillo, R. Gomperts, R. E. Stratmann, O. Yazyev, A. J. Austin, R. Cammi, C. Pomelli, J. W. Ochterski, R. L. Martin, K. Morokuma, V. G. Zakrzewski, G. A. Voth, P. Salvador, J. J. Dannenberg, S. Dapprich, A. D. Daniels, O. Farkas, J. B. Foresman, J. V. Ortiz, J. Cioslowski and D. J. Fox, Gaussian 09, Revision C.01, Gaussian, Inc., Wallingford CT, **2010**.

[2]A. D. Becke, *Physical Review A*, **1988**, *38*, 3098-3100.

[3]C. Lee, W. Yang and R. G. Parr, *Physical Review B*, **1988**, *37*, 785-789

[4]A. D. Becke, *J. Chem. Phys.*, **1993**, *98*, 5648-5652